

# A NEW PROGRAM TO CALCULATE THE TEXTURE VECTOR FOR THE VECTOR METHOD.

**A. Vadon**

Ecole nationale d'ingénieurs

LMPC. METZ University

Ile du Saulcy

57045 Metz. France.

**J. J. Heizmann**

Faculté des sciences

## 1. Introduction

The Vector Method is now well known<sup>1,2,3,4,5</sup> and has proved its efficiency especially for the analysis of sharp and medium textures. Yet, like any other method of analysis it can be improved thanks to the users' experience and to progress in the methods of numerical analysis and in the computers.

The improvements we intend to propose to-day are of two kinds :

—First a theoretical improvement : the calculation of the partial norm has been improved in the case of an analysis with several incomplete pole figures.

—Secondly, a practical improvement : the calculation process is more powerful.

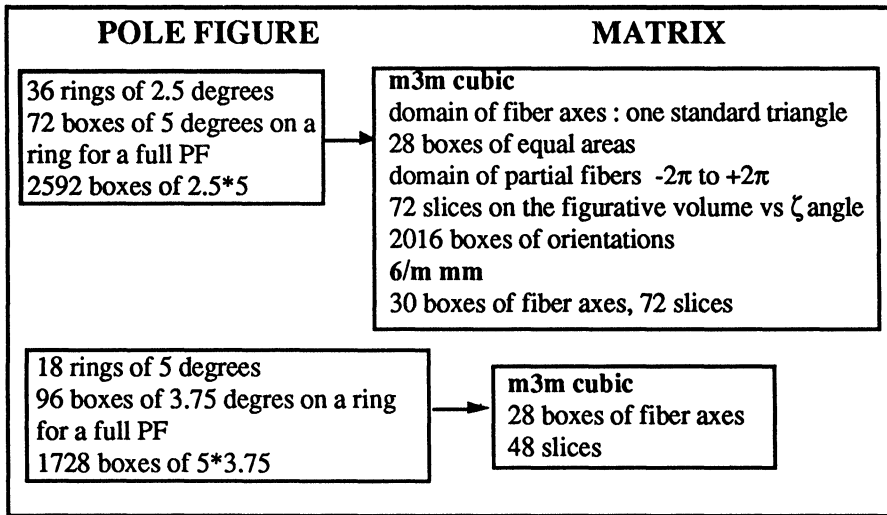
## 2. The old method and the new one

The Vector Method calculates the texture vector by a succession of iterations. Until recently the inversion was made with one, two or three complete or incomplete pole figures and by inverting the system :

$$(\mathbf{X}_k) = [\sigma_{pn}] (\mathbf{Y}_v)$$

### 2.1 Some common values

Here is an example of the treatment of an analysis for an m3m cubic crystal with three complete pole figures. Each pole figure is partitioned in 36 rings (2.5° in width) of 72 boxes each, or a total of 2592 boxes. The orientation space is discretized in 2016 boxes (28 boxes for the unit triangle and 72 cross-sections according to a rotation  $\zeta$ ). So each  $[\sigma_{pn}(hkl)]$  matrix is a matrix with 2592 rows and 2016 columns.



As there can be up to 3 matrices in juxtaposition, the whole set may seem enormous. Luckily each matrix is sparse (only 10% of non-zero terms)

$$\begin{pmatrix} x_1 \\ x_2 \\ x_3 \end{pmatrix} = \begin{bmatrix} h_1 \\ \sigma_{pn} \\ h_2 \\ \sigma_{pn} \\ h_3 \\ \sigma_{pn} \end{bmatrix} \quad (Y)$$

**In the old method** we started the iterations with an isotropic texture vector, i.e. having all its components equal to 1, the texture vector being normed according to the number of boxes in the partitioning of the orientation space.

If the figures are incomplete - and that is usually the case since we wish to avoid the complications of the reflection-transmission measurements - the number of rows of the matrix decreases. But a new problem arises : the problem of the normalization of the incomplete figures used.

To resolve the problem of normalization, we would use an approximate norm, calculated from the known portion of the Direct Pole Figure (the figure being normed according to the number of boxes explored and by taking into account the area scanned, so that each box had the value 1 when the explored portion of the pole figure was isotropic). The nearest the mean value of the intensities calculated on the known part is to the mean value calculated on the complete pole figure, the most accurate the approximate norm is. That is seldom the case, especially if the pole figures are very sharp. Still, the calculated solution is correct because the linear system is widely over-dimensioned. Thus, with 3 incomplete pole figures limited to  $75^\circ$  (30 rings of  $2.5^\circ$  each) the matrix has  $3 \times 30 \times 75 = 6480$  rows for only 2016 columns or 2016 texture vector components.

**In the new method** we have tried to resolve better the problem of incomplete norm and at the same time improve the efficiency of the algorithm. The basic idea is to invert first the axial figures, complete or not, before making the inversion which gives the texture vector itself.

The density of fiber axes being known, the experimental figures can be normed more accurately. Moreover, the density of fiber axes represents the mean value of the texture components belonging to the fiber. The iterations for the inversion of the texture vector can be started with that mean value.

### 3. Calculation of the axial texture vector

The Direct Pole Figures are first axialized about the normal to the sample by just summing the Direct Pole Figure intensities on each ring. If  $(X_p)_i$  represents the Direct Pole Figure vector of the  $i$ th figure we note  $(X_k^*)_i$  the corresponding Axial Pole Figure vector. From an Axial Pole Figure we can calculate the intensity of fiber axes  $Y^*$  by a linear relation identical to that of the figure inversion, provided the corresponding axial matrix is used.

$$(X_k) = [\sigma_{p n}](Y_n)$$

$(X^*)$  is the the axial pole figure composed of  $k$  components,  $k$  being the number of rings on the Direct Pole Figure,  $\sigma_{kv}$  is the axial matrix ( $k$  rows and  $v$  columns) and  $Y^*$  the axial texture with  $v$  components.

The inversion of this relation is made with the number of incomplete figures we have at our disposal (generally 1 to 4). We can note that because of the blind central area obtained during the measurement of the Direct Pole Figure components which are not in the BRAGG position on our multifigure goniometer<sup>6,7</sup> we have planned in the numerical treatments the possibility of treating incomplete figures as well at the periphery as at the center. At this point I can mention that the results obtained during an analysis are nearly always better when the central ring is suppressed. This fact is easily understood: The measurement of the central area is made with important errors because the sample rotates and the section of the X ray incident beam is much larger than a box on the first ring.

The inversion of the Axial Pole Figure is far easier than the inversion of the Direct Pole Figure. The matrices are small (for the m3m cubic system: 36x28) and they are sparse. Some tests are then possible on the matrices, for instance a test of good conditioning. Besides, the treatment is very fast (1 second by iteration with a 16 MHz processor). So it is easy to do 100 to 150 iterations, which allows to analyse the stability of the residu (to know if the convergence is good or on the contrary if there is a fluctuation between 2 limits). The fluctuation of a residu generally proves that the pole figures are not good. (They are inconsistent with one another or inconsistent in themselves). As the Vector Method uses directly the correlations between areas belonging to the same orientation (so-called elementary pole figures) a bad inter-

correlation on one or several figures or between 2 figures stops the calculation process : it fails to converge and gives a strong residu.

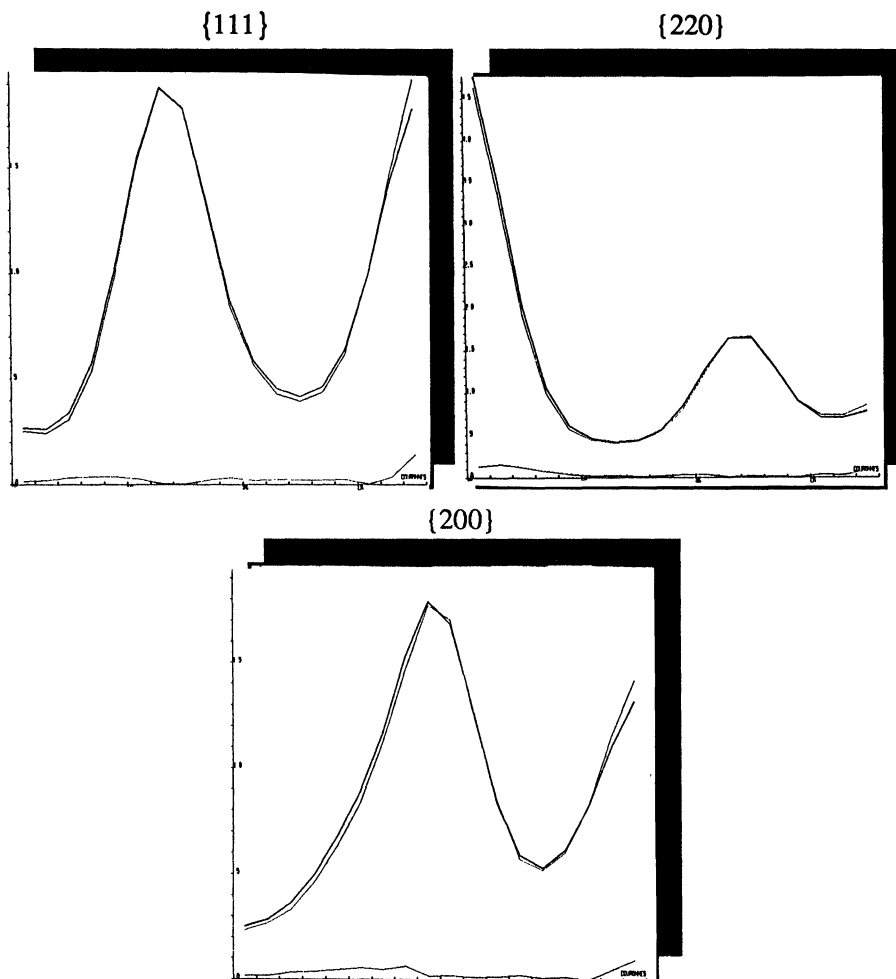
### An example of axial analysis

with 3 complete Direct Pole Figures given by ORSAY Laboratory (R. Pennelle) and obtained in neutron transmission. The partitioning was :18 five-degree rings, 96  $3.75^\circ$  boxes for each ring. The figures were figures  $\{111\} + \{220\} + \{200\}$  treated at the same time. We obtained the following results :

- 5 iterations by second
- the residu was stable : 3.41 % already after the 22nd iteration.

Even though we carried the iterations as far as 150, the values of the residus,  $Y^*_{max}, Y^*_{min}$  remained absolutely stable.

Here are 3 pictures, each of them showing the 3 curves of the experimental, calculated and residual axial pole figures for the 3 axial poles figures.



The experimental axial figure is practically superposed to the recalculated figure.

Here are the “standard” errors : E1-0.01 is the mean deviation of order 1 on all the values over 0.01 and so on, E2 is the mean deviation of order 2 and RP the mean relative error. The very small values confirm the good superposition of the curves.

ERRORS	FP{111}	FP{220}	FP{200}
E1-0.01	2.87	3.14	4.63
E1-0.5	3.19	3.33	5.20
E2-0.01	4.10	3.91	6.39
E2-0.5	4.75	4.20	6.95
RP-0.1	4.03	4.12	3.87
RP-0.5	2.90	3.25	3.84
RP-1.0	2.55	3.30	3.05

#### 4. Calculation of the vector texture Y.

##### 4.1. Improvement of the norm for the calculation of Y

The axial texture vector  $Y^*$  is normed according to the number of fiber axis boxes. The same norm coefficient allows to norm the figures taking part in the analysis. Besides, the normed Axial Pole Figure will serve to adjust the Direct Pole Figure. The flow of normals to the sample penetrating the explored area of the pole figure must be the same on the Axial Pole Figure and the Direct Pole Figure.

This allows to correct each value of the Direct Pole Figure. Thus, the values of the Direct Pole figure explored are adjusted to the norm found for  $Y^*$ .

**Example :** In the last example, the norm coefficient of  $Y^*$  is 0.988. It should be 1.000 since the pole figure is complete. The 3 coefficients to correct the three PFD {111}, {200}, {220} are respectively 1.002, 1.003, 1.003 instead of 1. In the case of incomplete figures the coefficients may reach 0.7 or even 0.6.

##### 4.2. Calculation of Y

It is calculated from the adjusted Direct Pole figures. Moreover, the initial texture vector, at iteration 0, is no longer the isotropic texture vector ( $Y_i = 1$  from  $i=1$  to  $i=2016$ ) but a texture vector in which each component has for value the value of the corresponding axial pole figure component.  $Y_k^*$  represents the mean value of the texture components belonging to the same axial figure. Starting at this point reduces the computing time, all the more so when the texture shows one complete central fiber.

**Example :** continuation of the previous analysis.

The next 3 double pictures show the experimental and recalculated direct pole figures for the 3 poles figures {111}+{220}+{200} used for the analysis.

